

3.1 Materials

In this investigation, RHA was used as the primary waste ingredient for silica source. ES and seashell were utilized as calcium oxide sources, and FA was employed as the combination of alumina and silica source. Other wastes, like river silt and refractory grog were also incorporated to increase the amount of wastes in the composition for the fabrication of ceramics. Before using these wastes as raw materials, some treatments like washing, drying, and heat-treatment were performed for reducing the impurity level. The grinding process was also executed with different time and rpm values for different wastes to reduce the particle size. The wastes were selected according to the particular ceramic composition, and the amount of the waste incorporation into the selected composition was optimized through the number of trails. The fabrication process for the particular ceramic was selected through the trail of different methods, and the easy, economical route was adopted for the sustainable ceramic fabrication.

3.1.1 Rice husk ash

RHA was collected from a local rice mill (Samrat rice mill, Burdwan, India), where rice husk was often used as a fuel. This RHA contained a trace amount of volatile matter as well as carbon. To eliminate the carbon, the RHA was heat-treated further at 700°C for 2 h. Later, the dry milling was then conducted in a ball mill (Model No: MBM-07, Insmart Systems, Hyderabad, India) using high purity zirconia balls of 5 mm diameter for about 30 min at 300 rpm in water as a medium with a weight ratio of balls to the powder of about 5:1. The chemical composition of the RHA and heat-treated RHA were analyzed using X-ray fluorescence (XRF) (Philips PW 2400, Netherlands) spectrometer shown in [Table 3.1](#). The RHA and heat-treated RHA contained 90.13 wt.% and 93.20 wt.% of SiO₂, respectively. [Figure 3.1\(a\)](#) shows the X-ray diffraction (XRD) curve of heat-treated RHA. The measurements were performed on a “Rigaku Desktop Miniflex II X-Ray Diffractometer” equipped with Ni filter and Cu- α (1.5406 Å) radiation in the range from 10° to 70° with a step size of 0.02° and scanning rate 2°/min (Model No: HD20972, Rigaku Corporation,

Tokyo, Japan). The absence of any sharp peak demonstrated that the silica in the RHA was in amorphous form only. Figure 3.2 (a) shows the scanning electron microscopy (SEM) image of the heat-treated and grounded RHA. SEM analysis was carried out using a scanning electron microscope (FEI, Nova Nano SEM 450, Netherlands) after gold coating on the surface of RHA powder through a gold sputter coating instrument. The secondary electron's image of the sample was collected for topography information of RHA particles. The particles were irregular-shaped, and the average size was 1.20 μm , as estimated from the SEM micrograph using “Image J1.48V” software.

Table 3.1 Chemical composition of waste ingredients.

Compound (wt.%)	RHA	Heat-treated RHA	Calcined eggshells	River silt	Fly ash	Calcined seashells	Refractory grog
SiO ₂	90.13	93.20	-	72.51	54.49	0.23	62.71
Na ₂ O	2.52	2.86	0.17	2.04	0.91	0.17	1.32
P ₂ O ₅	1.08	1.18	0.23	0.10	-	-	-
K ₂ O	1.02	1.12	-	2.40	0.68	0.15	0.87
CaO	0.43	0.52	99.08	1.71	11.47	98.85	-
Fe ₂ O ₃	0.31	0.35	0.08	3.25	1.16	0.13	1.49
TiO ₂	0.26	0.31	-	0.43	1.24	-	0.92
MgO	0.22	0.27	0.29	1.32	1.07	0.21	0.52
Al ₂ O ₃	-	-	-	10.99	26.34	0.26	32.17
SrO	-	-	0.15	-	-	-	-
RuO ₂	0.17	0.19	-	-	-	-	-
L.O.I	3.86	-	-	5.25	2.64	-	-

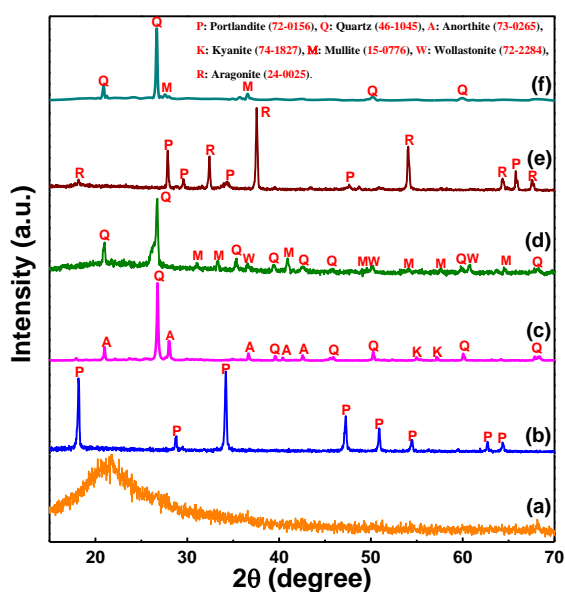


Figure 3.1 XRD patterns of (a) heat-treated RHA, (b) heat-treated eggshell, (c) river silt, (d) fly ash, (e) heat-treated seashell, and (f) refractory grog.

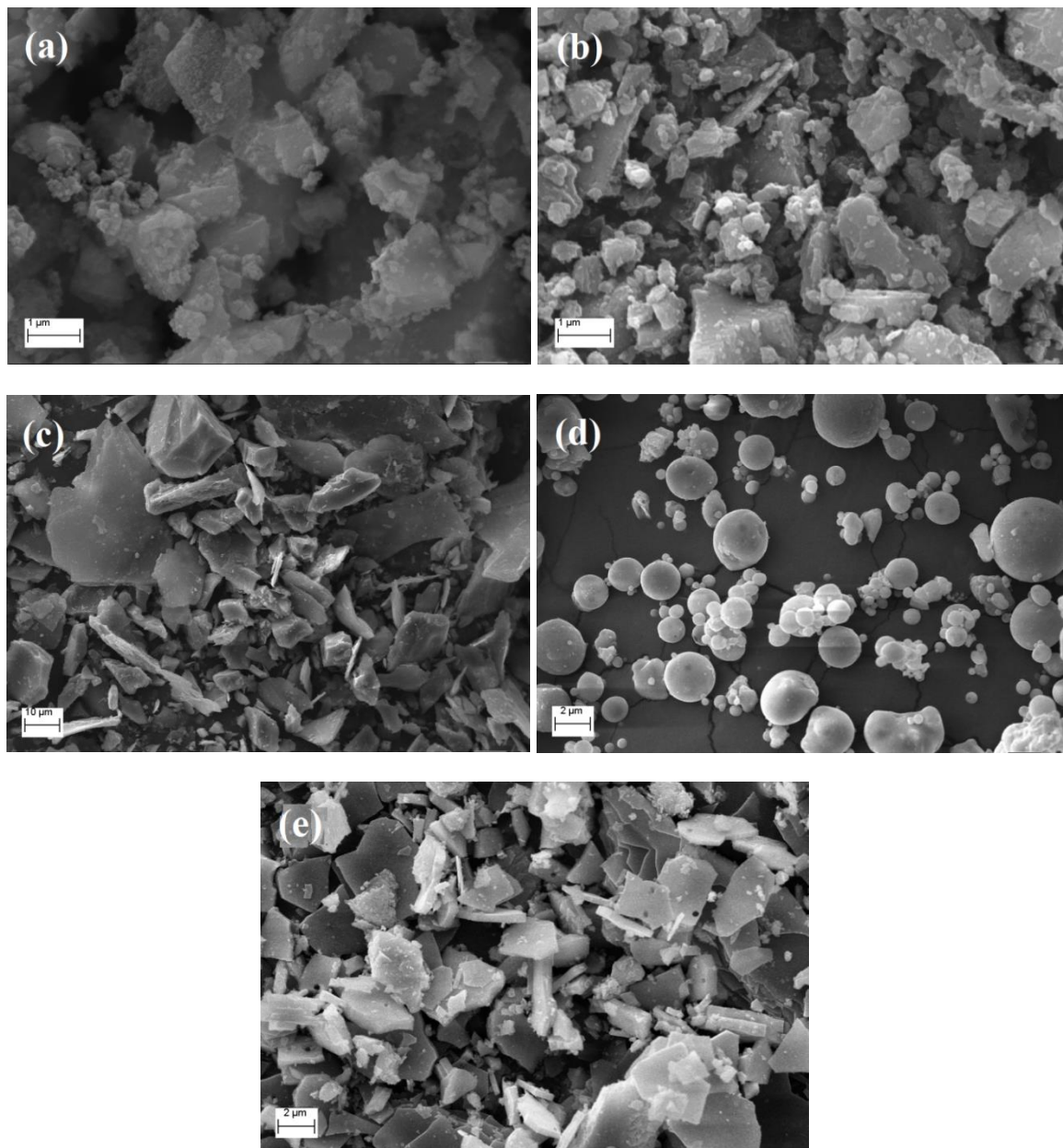


Figure 3.2 SEM images of (a) grounded heat-treated RHA, (b) grounded heat-treated eggshell, (c) grounded river silt, (d) fly ash, and (e) grounded heat-treated seashell.

3.1.2 Eggshell

Eggshells were collected from a nearby restaurant. They were cleaned in DI water and dried in sunlight. Later, the shells were initially crushed using a domestic mixer, and dry milling was then conducted in a ball mill for about 30 min at 300 rpm with a weight ratio of balls to the powder of about 5:1. The milled mass was then calcined at 950°C for 2 h in an air atmosphere. [Table 3.1](#) represents the chemical composition of the calcined eggshells. It was found that the powder contained greater than 99% of CaO. However, the calcined eggshell powder was composed mainly of portlandite [Ca(OH)₂], which was confirmed by the XRD

studies, as shown in [Figure 3.1\(b\)](#). The formed phase was identified with the help of Philips X-pert high score software, which was based on the Hanawalt method and matched with “JCPDS International Centre for Diffraction Data Cards.” The portlandite was probably formed by the absorption of moisture from the atmosphere by calcium oxide (CaO). A similar phenomenon was observed by [Leite *et al.* \(2017\)](#). [Figure 3.2\(b\)](#) exhibits the particle morphology of the calcined eggshell powder. The powder was composed mainly of uneven shape particles with an average particle size of 0.50 μm .

3.1.3 River silt

Silts were collected from Kosi River, Bihar, India, and washed in water to remove any water-soluble impurities. Later, the silts were wet milled, using water as milling media in a ball mill for about 4 h with 300 rpm with a weight ratio of balls to silts of 5:1. The composition of the silt is shown in [Table 3.1](#). It consisted mainly SiO_2 , Al_2O_3 , Fe_2O_3 , Na_2O , K_2O , CaO , MgO along a trace amount of TiO_2 , and P_2O_5 . [Figure 3.1\(c\)](#) represents the XRD pattern of grounded silts. The presence of crystalline phases of quartz (SiO_2), anorthite ($\text{CaAl}_2\text{Si}_2\text{O}_8$), and kyanite (Al_2SiO_5) were detected from the pattern. [Figure 3.2 \(c\)](#) displays the particle morphology of the grounded silts. The silt powder was composed mainly of irregular-uneven shaped particles and the average size around $\sim 9.70 \mu\text{m}$, enumerated from SEM image. [Figure 3.3 \(a\)](#) shows the differential thermal and thermo-gravimetric analysis (DTA–TGA) curve of the river silt. DTA–TGA was carried out for the river silt in an air atmosphere with a heating rate of $5^\circ\text{C}/\text{min}$ using “KEP-Technologies, Setaram-Scientific & Industrial Equipment, France (Model-Labsys, Serial no-560/51,920).” Around 10 mg of silt powder was taken for this investigation, and $\alpha\text{-Al}_2\text{O}_3$ was used as a reference sample. The plot ([Figure 3.3 \(a\)](#)) shows the information about the change of weight and the enthalpy of the sample as a function of temperature. First weight loss ($\sim 3.65 \text{ wt.}\%$) was observed with increasing temperature up to 700°C due to the combined effect of burning organic components and loss of the adsorbed water from the silts. It was attributed to a wide range of low-intensity exothermic peak (100°C to 700°C). Then, endothermic peak (heat absorption)

might be due to the decomposition of carbonate present in silts. It was attributed to the ~1.5 wt.% of weight losses.

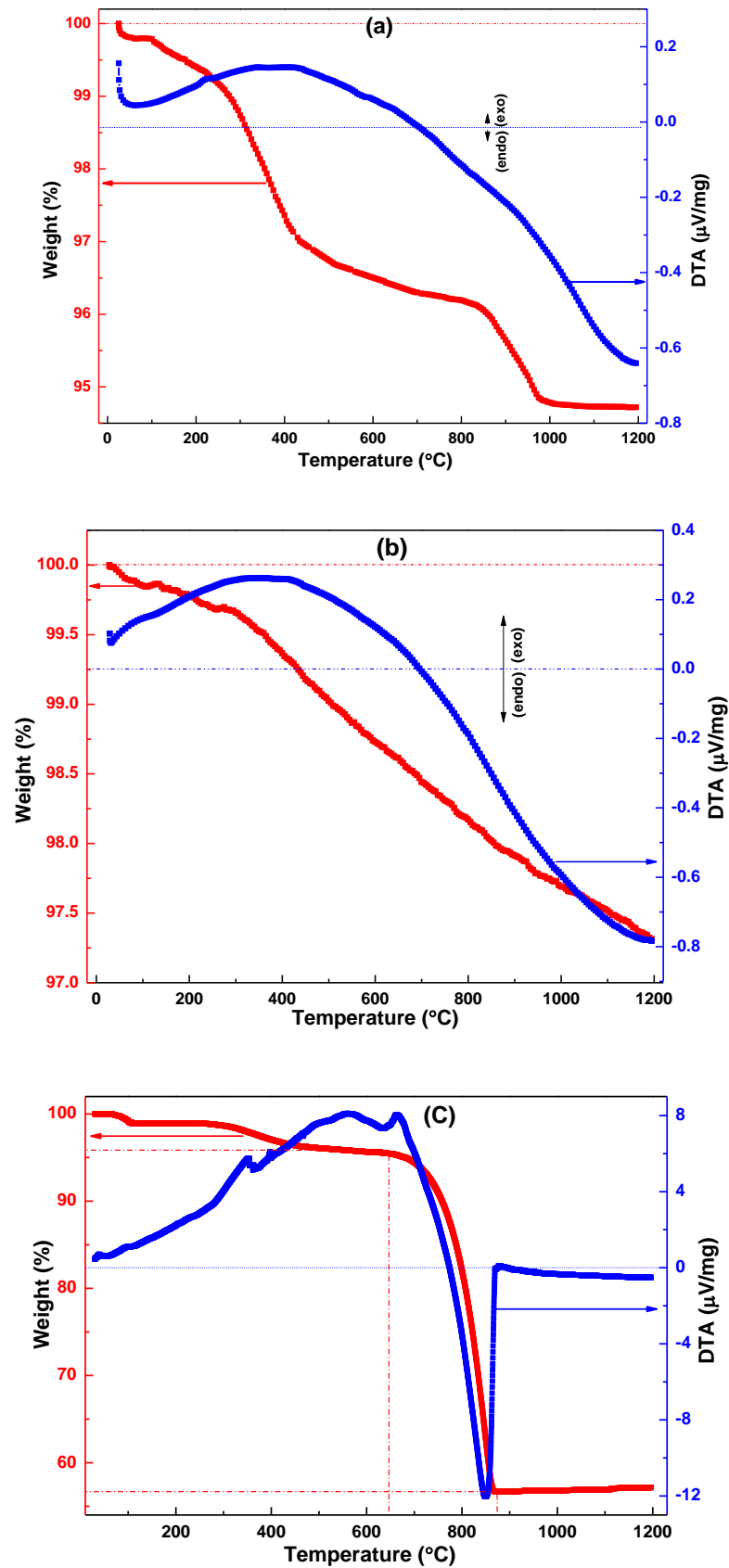


Figure 3.3 DTA-TGA curves of (a) river silt, (b) fly ash, and (c) seashell.

3.1.4 Fly ash

Fly ash was collected from National Thermal Power Corporation, India. The chemical composition of fly ash is presented in [Table 3.1](#). It contained SiO₂ (54.49 wt. %), Al₂O₃ (26.64 wt. %), and CaO (11.47 wt. %) as major components and minor components, i.e., Na₂O, K₂O, Fe₂O₃, MgO, and TiO₂ were less than 7.4 wt.%. [Figure 3.1\(d\)](#) shows the room temperature XRD analysis of the fly ash. It indicated the presence of crystalline phases of quartz (SiO₂), mullite (Al₆Si₂O₁₃), and wollastonite (CaSiO₃). [Figure 3.2\(d\)](#) exhibits the particle morphology of fly ash. The fly ash particles were mostly spherical in shape with a smooth surface, and the average particle size was around 4.40 μm. [Figure 3.3 \(b\)](#) shows the DTA and TGA curve of fly ash up to 1200°C in an air atmosphere. A little weight loss was detected with increasing temperature (~2.7 wt.% up to at 1200°C) due to the combustion of unburnt carbon. It was ascribed to a wide range of exothermic peak up to 700°C, and then the endothermic peak was observed due to the decomposition of carbonates.

3.1.5 Seashell

Seashells (oyster, snail, clam, and mussel) were collected from the fishery market of Digha, India, where it was available abundantly. At first, shells were cleaned in tap water and then dried at room temperature (25°C). Initially, shells were crushed by steel aged-mortar, and then milling was performed in a ball mill for 1 h at about 300 rpm with material to ball weight ratio 1:5. The milled mass was then heat-treated at 900°C in air atmosphere. [Table 3.1](#) illustrates the chemical composition of a heat-treated seashell, which contained above 98 wt.% of CaO. The heat-treated seashell was composed of calcium oxide (CaO) and portlandite (Ca(OH)₂), which was confirmed by the XRD analysis shown in [Figure 3.1\(e\)](#). Most probably, the portlandite was formed through the absorption of moisture from the atmosphere by calcined seashell (~98 wt.% CaO). [Figure 3.2\(e\)](#) shows the SEM image of heat-treated seashells powder. It consisted mainly of irregular-shaped particles with an average particle size of around 1.30 μm. The DTA-TGA curve for the grounded seashell up to 1200°C is shown in [Figure 3.3\(c\)](#). In the TGA curve, around 4 wt.% of weight loss was detected in the

temperature range from 80°C to 650°C due to the removal of absorbed and combined water, and burning of organic compounds, i.e., proteins, polysaccharides, and glycoproteins presented in the seashell, (García *et al.*, 2017). Therefore, a wide range of exothermic peaks was observed in the DTA curve. At high temperature, around 650 to 880°C a large endothermic peak was detected due to the decomposition of CaCO₃ ($CaCO_3 = CaO + CO_2$), which was also contributed to the huge amount of weight loss (~40 wt.%). On the other hand, 100% pure CaCO₃ was associated 44 about wt.% of weight loss in this region. However, the seashell showed only 40 wt.% of weight loss in the CaCO₃ decomposition region, which indicated that the seashell contented around 91 wt.% of CaCO₃. A similar phenomenon was observed by García *et al.* (2017). However, a total 44 wt.% of weight loss occurred up to 880°C, and then no further significant changes were observed up to 1200°C.

3.1.6 Refractory grog

Fired refractory grogs (waste fired refractories) were collected from the refractory industry. At first, grogs were crushed and then ball milled in a dry condition for 10 min at about 300 rpm with the ball to material weight ratio 5:1. The chemical composition of the grogs is shown in Table 3.1. It contained silica as a major component. The typical XRD pattern of grogs is shown in Figure 3.1(f). It retained a mainly crystalline form of silica and mullite.

3.1.7 Other materials

Analytical grade (AR) hydrochloric acid (assay 35%), sodium hydroxide plates (assay 99%), reactive alumina (assay 99 %), and calcined alumina (assay 99 %) were bought from Loba Chemie Pvt. Ltd., India. Blast furnace slag (BFS) was supplied by the steel industry (Sail, India). The calcium alumina cement (CAC) (CA-25M) and brown tabular alumina (98.16% Al₂O₃) were purchased from Almatiss, India, and S.D. Fine Chem. Ltd., India, respectively. The distilled water was used for all the synthesis process. Ball clay, feldspar, and quartz were purchased from Ace Cone Ceramics Ltd., Bikaner, India, and sieved through 90 µm sieves. All the raw materials were passed through the magnetic separator to eliminate any

iron particles present in the ingredients. Ordinary Portland Cement (OPC 43 grade) was purchased from ACC Limited, India. The chemical composition of tabular alumina, CAC, BFS, quartz, ball clay, feldspar, and OPC are tabulated in [Table 3.2](#).

Table 3.2 Chemical composition of tabular alumina, CAC, BFS, quartz, ball clay, feldspar and OPC.

Compound (wt.%)	Tabular alumina	CAC	BFS	Quartz	Ball clay	Feldspar	OPC
SiO ₂	0.76	0.30	35.42	98.66	52.37	65.92	20.49
Na ₂ O	0.17	0.80	-	0.15	0.72	1.86	0.42
K ₂ O	-	-	-	0.14	1.84	12.22	0.53
CaO	-	18.10	40.67	0.08	0.86	0.56	65.47
Fe ₂ O ₃	0.49	0.20	0.45	0.12	2.06	0.43	3.87
MgO	-	0.40	6.83	0.09	0.23	0.26	1.67
P ₂ O ₅	-	-	0.13	0.06	-	0.34	-
Al ₂ O ₃	98.16	80.20	14.52	0.24	29.86	17.24	5.76
S	-	-	1.23	-	-	-	-
MnO	-	-	0.73	-	-	-	-
TiO ₂	0.42	-	-	0.08	0.08	0.32	-
L.O.I	-	-	-	0.38	11.98	0.87	1.69

3.2 Synthesis and characterization of the ceramics

3.2.1 Silica and silica sol

The preparation flow chart of the silica and silica sol from RHA are shown in [Figure 3.4](#). The as-collected RHA, passed through 90 µm sieve, was first cleaned at room temperature with 0.5 N HCl solutions with continuous stirring for 30 min to remove any possible metal impurities or dirt's. 0.75 weight ratios of clean RHA and NaOH pallet was mixed with the distilled water (1 lt. water with 100 g mixture) in a glass beaker at 90°C for 1 h. For completion of the reaction ([reaction 3.1](#)), the mixture was left for 24 h at room temperature. The unreacted solid part was separated from the sodium silicate solution through millipore filter papers. The filtrated silicate solution was slowly acidified by the addition of HCl under constant stirring until the transparent solution was completely precipitated into a white silica gel ([reaction 3.2](#)). The gel was left for aging for 1 day, and then repetitively washed through the deionized water to eliminate the Na⁺ or other ions. The acquired product was then controlled (time and temperature) heat-treated in an air oven to remove excess free water. For silica, the obtained product was then dried at 110°C for 12 h and ground into fine

white silica powder. Different solid containing sols (7.5 wt.% and 30 wt.%) were prepared by controlled (time) heat-treatment at 80°C. The efficiency of this method was around 70%. The following reactions took place during the silica extraction from the RHA:

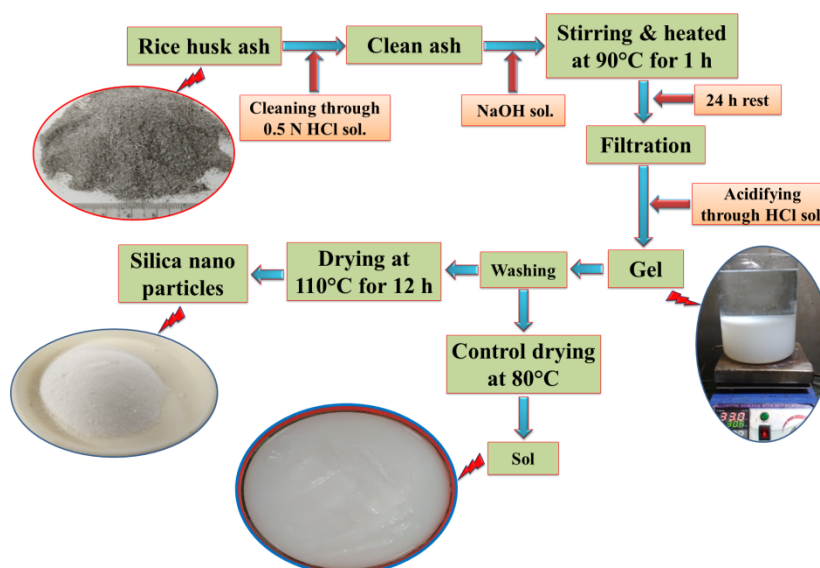
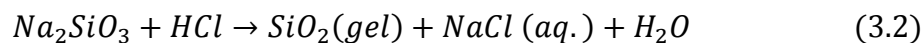
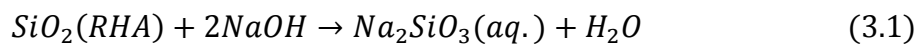


Figure 3.4 Preparation flowchart of RHA derived silica and silica sol.

The RHA derived silica powder was characterized by XRD, Fourier transform infrared spectroscopy (FTIR), SEM-EDX, transmission electron microscopy (TEM), and DTA-TGA. FTIR analysis was performed to confirm the type of bonding present in the materials through transmittance mode. The spectra were recorded by the attenuated total reflection (ATR) method at room temperature in between 4000-400 cm^{-1} with BRUKER (TENSOR 27-3772, Kanagawa, Japan) infrared spectrometer. The particle morphology and internal structure of silica powder were examined through transmission electron microscopy (TEM) (FEI, TECNAI G2-20 TWIN, Eindhoven, Netherlands). First, a small amount of silica powder was mixed with an ethanol solution and then ultrasonicated for 20 min. After that, a single drop from the middle level of the silica mixed solution was put on the copper grid and dried at 50°C for 1 h in an air oven. This silica particle stacked grid was used for the TEM analysis. Images were collected from both TEM moods, i.e., imaging and diffraction. This silica

powder was used for the fabrication of ceramic foams (silica and mullite) and castable refractory.

3.2.1.1 Silica foam

The preparation process of silica foam is described in [chapter 4](#). Different physico-mechanical properties like phases, apparent porosity (AP), bulk density (BD), cold crushing strength (CCS), microstructure, surface area, pore size, and volume were analyzed of prepared silica foam.

AP and BD of the foam samples were measured using Archimedes' method based on [ASTM C20 \(2010\)](#). Distilled water was used as buoyancy liquid, and all the weights were measured through 0.0001 gm accuracy weighing balance with a density measurement kit. The AP was measured through the following equation:

$$AP (\%) = \frac{W_s - W_d}{W_s - W_a} \times 100 \quad (3.3)$$

where, W_d is dry sample weight, W_s is the weight of the sample after soaking in water, and W_a is the suspended weight of the sample. The BD was measured by the following equation:

$$BD = \frac{W_d}{W_s - W_a} \quad (3.4)$$

[ASTM C133 \(2015\)](#) defined method was applied to determine the cold crushing strength (CCS) of foam specimens by Universal Testing Machine (Tinius Olsen, Noida, India, H10KL-I0129). For the appropriate result of CCS, six specimens of each sample were tested. CCS was calculated through the following equation:

$$CCS = \frac{F}{A} \quad (3.5)$$

where, F is applied load (N), and A is area (mm^2).

The Brunauer-Emmett-Teller (BET) surface area (S_{BET}) and nano-pore characteristics (volume and avg. diameter) of the foam sample was measured by ASAP® 2020 Plus: Accelerated Surface Area and Porosimetry System (Micromeritics Instrument Corp., United States) after a pre-examination treatment at 100°C for 2 h.

3.2.1.2 Mullite foam

RHA derived silica sol (7.5 wt.% solid) with reactive alumina was used to synthesize mullite foam specimens. The preparation method is described in [chapter 5](#). The rheological behaviour of the slurry for slip casting was characterized through a stress-controlled rheometer (MCR 72, Anton-Paar, GmbH, Austria) with a concentric cylinder measurement geometry and viscosity, which were determined under the continuous increasing shear rate from 0.01/s to 100/s at room temperature. Different properties like AP, BD, phases, microstructure, CCS and thermal conductivity (κ) of foam samples were analyzed.

The κ of samples was measured by the hot cross-wire method using “thermal conductivity measurement apparatus, VBCC, LOC: 441A102-0005.” It could be defined as the amount of heat conducted through material in unit time, per unit temperature gradient towards the direction of flow and unit cross-sectional area of material, i.e., defined according to the following equation ([Mitsubishi, 2005](#)):

$$q = -\kappa \frac{dT}{dx} \quad (3.6)$$

where, q is the heat flow per unit time per unit area (W/m^2), κ is the thermal conductivity ($\text{W}/\text{m}\cdot\text{K}$), and dT/dx is the temperature gradient through the material.

3.2.1.3 Castable refractory

RHA derived silica and silica sol (30 wt.% solid) were used with other ingredients (different types of alumina and CAC) to synthesize castable refractory. The preparation method is described in [chapter 6](#). Different physico-mechanical properties like AP, BD, bending strength (BS), CCS, hot modulus of rupture (HMoR), thermal shock resistance (TSR), and blast furnace slag (BFS) corrosion resistance test were performed. Three-point bending strength (BS) was determined according to the method defined in ASTM C133 (2015) by Universal Testing Machine (Tinius Olsen, Noida, India, H10KL-I0129). 50 mm length \times 10 mm width \times 5 mm thickness specimens were used for the BS test. Six specimens

of each composition were tested for appropriate results and test was performed at room temperature. BS was calculated through the following equation:

$$BS = \frac{3FL}{2bd^2} \quad (3.7)$$

where, F is the breaking load (N), L is the length (mm), d is thickness (mm) and b is width (mm). The testing setup is graphically represented in Figure 3.5.

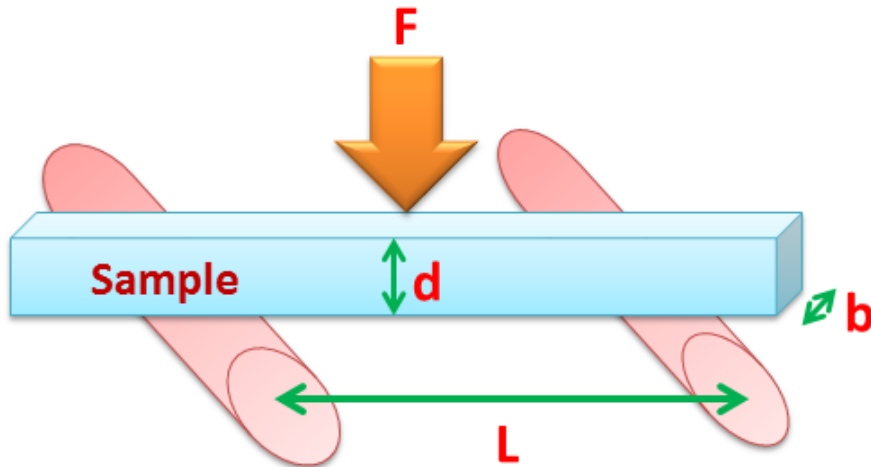


Figure 3.5 Testing setup of bending strength.

The HMoR of the fired castable specimens was determined at 1400°C in air atmosphere according to ASTM C583-10 (2015) in a HMoR furnace (Bysakh & Co, Kolkata, India). The testing mechanism was the same as BS testing but it was performed at high temperature furnace.

Thermal shock resistance (TSR) of the fired castable samples was examined by the measurement of CCS values after repetitively air quenching from 1200°C to ambient temperature. The fired castable specimens were heat-treated at 1200°C for 15 min and air quenched at room temperature for 10 min. This event was repeated, and CCS was measured at a regular interval of 2 cycles.

For BFS corrosion resistance, the central groove (10 mm diameter and 15 mm height) of the fired castable blocks were used, and BFS powder was poured into the groove. The melting was done in a muffle furnace at 1500°C for 30 h. The blocks were then cut into

vertically by diamond cutter and the castable-BFS interface was examined by SEM and energy dispersive X-ray (EDX)-mapping techniques.

3.2.2 Wollastonite

The preparation flow chart for wollastonite is shown in Figure 3.6. Wollastonite powder with the general formula $\text{CaO}\cdot\text{SiO}_2$ was prepared by the solid-state reaction method using a stoichiometric (1:1 molar) amount of calcined eggshells (~99% CaO) and heat-treated RHA (~93% SiO_2) as ingredients. Two respective powders were wet ball-milled in water media for 4 h at 600 rpm. The mixture was then dried at 110°C and calcined at four different temperatures, i.e., 1000, 1100, 1150 and 1200°C, for 2 h in an air atmosphere. The agglomerate calcined particles were then dry-milled for 30 min at 300 rpm. Wastes derived wollastonite powders were characterized through the XRD, FTIR, and SEM. The prepared powders were used to further synthesizing of wollastonite bodies and tiles.

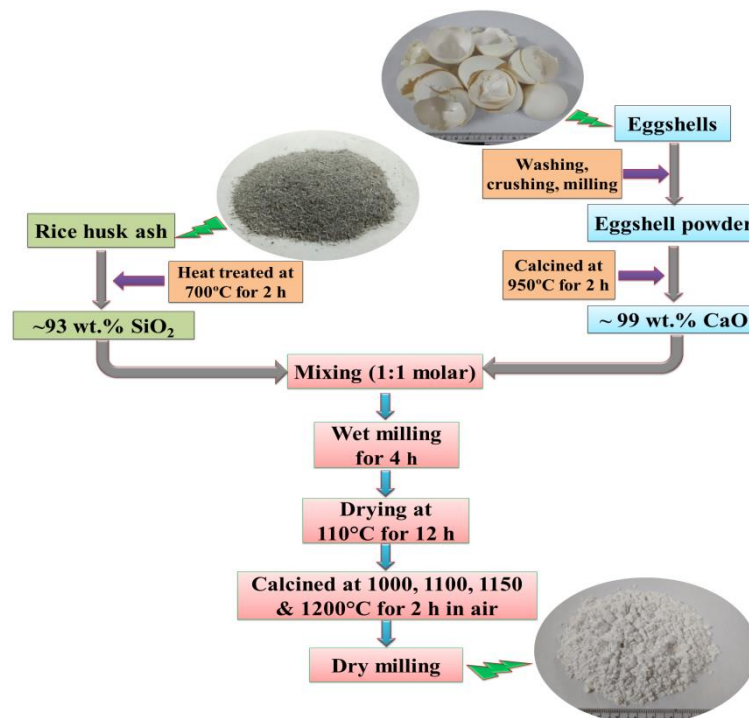


Figure 3.6 Preparation flowchart of synthetic wollastonite.

3.2.2.1 Wollastonite ceramic

AP, BD, BS, phases, microstructure and dielectric properties of wollastonite ceramics (sintered wollastonite) were deeply investigated. The high-purity silver electrode paste was coated on two surfaces of sintered wollastonite pellet and cured at 150°C for 2 h for dielectric

properties measurement using Impedance analyzer (Key Sight Technology, Model-E4990A, Malaysia). The dielectric constant (ϵ') and AC resistivity (ρ) were evaluated through [equation 3.8](#) and [3.9](#), respectively.

$$\epsilon' = \frac{cd}{A\epsilon_0} \quad (3.8)$$

$$\rho = \frac{1}{\omega\epsilon_0\epsilon'tan\delta} \quad (3.9)$$

Where, c = capacitance, d = sample thickness, A = sample area, ϵ_0 = the permittivity of free space (8.85×10^{-12} F/m), ω = the angular frequency ($2\pi f$), f = linear frequency and $tan\delta$ = dissipation factor. The dielectric constant, loss angle tangent and resistivity of the wollastonite had been plotted with frequency. The working temperature of waste-derived wollastonite was measured through the heating of samples at room temperature to 600°C at a rate of $1^\circ\text{C}/\text{min}$ with 1 MHz frequency.

3.2.2.2 Tile

Tile samples were prepared through the replacement of quartz and feldspar by the river silt and waste-derived wollastonite, respectively. The preparation process is described in [chapter 7](#). The densification mechanisms, phases, surface morphology, AP, BD, water absorption (WA), shrinkage, BS, CCS, and chemical resistance were comprehensively examined. WA of the tile samples was determined according to [ASTM C20](#). The WA was measured through the following equation:

$$WA (\%) = \frac{W_s - W_d}{W_a} \times 100 \quad (3.10)$$

The linear shrinkage or expansion (LS) of the sintered sample was determined by the following equation:

$$LS(\%) = \frac{l_g - l_f}{l_g} * 100 \quad (3.11)$$

where, l_g and l_f is the linear length of green and fired samples, respectively and loss on ignition (L.O.I) was measured by the following relation:

$$L. O. I(\%) = \frac{w_g - w_f}{w_g} * 100 \quad (3.12)$$

where, w_g and w_f is the weight of green and sintered samples, respectively.

The acid-alkali resistance test of tiles specimens was performed according to [ASTM C650-04 \(2014\)](#). The experiment was done in a laboratory atmosphere. 10% HCl and 10% KOH solutions were used as testing fluids. The testing faces of ceramic tile pieces were dipped in the acid or alkali solution for 24 h and then examined through necked eye. Several marks were drawn across the specimen with the pencil in the treated areas. These pencil lines were removed with the damp-cloth.

3.2.3 Ceramic board

First, the multi-phase ceramic powder (MCP) was synthesized by using fly ash and heat-treated seashell as ingredients. Then, prepared powder was examined through XRD, FTIR, and SEM. The MCP was used with ungrounded rice husk ash (URHA), RH and OPC for the fabrication of ceramic board (preparation process of MCP and board are discussed in [chapter 8](#)). AP, BD, WA, BS, CCS, phases, microstructure, thermal conductivity, and humidity effect on strength were investigated.

Expansion of ceramic board samples in water was also measured after dipped in drinking water for 24 h at room temperature by the following equation:

$$v_e(\%) = \frac{v_a - v_b}{v_b} \times 100 \quad (3.13)$$

where, v_e , denotes expansion (%); however, v_b and v_a denote before and after volume of dipped samples, respectively.

The effect of humidity was analyzed after 28 days of sample preparation (OPC to take around 28 days for complete reaction) through “National Humidity Chamber”, India. The specimens were kept in a humidity chamber for 72 h with 50°C temperature and 80% of relative humidity atmospheric conditions, and then the strength (CCS) was determined. The humidity effect (HF) was estimated by the following equation:

$$HF(\%) = \frac{c_a - c_b}{c_b} \times 100 \quad (3.14)$$

where, c_b and c_a are the before and after CCS values of humidity treatment samples, respectively.

3.2.4 Insulation refractory

The insulation brick specimens were prepared with the combination wastes like FA, RHA, RH, and refractory grog. The synthesizing process of wastes derived insulation brick is discussed in [chapter 9](#). The important characteristics like AP, BD, phases, microstructure, BS, CCS, and thermal conductivity were deeply investigated for the insulation refractory.

The background and the synthesized procedure of the waste derived ceramics are discussed in their respective chapter. The findings from the characterizations of waste derived ceramics by the different techniques are also deeply studied, which are described in their particular chapter.